**Electronic Supplementary Information**

**for**

# Ni-PC@SBA-15 derived from nano-sized Ni-MOF-74 confined in SBA-15 as highly active catalyst for gas phase catalytic hydrodechlorination of 1,2-dichloroethane

Xin Ning,[a, b] Dongzhi Deng,[a] Heyun Fu*,[a] Xiaolei Qu,[a] Zhaoyi Xu,[a] Shourong Zheng[a]

[a] *State Key Laboratory of Pollution Control and Resource Reuse, School of the Environment, Nanjing University, Nanjing 210046, China*

[b] *Jiangsu Key Laboratory of Environmental Material and Engineering, School of Environmental Science and Engineering, Yangzhou University, Yangzhou 225000, China*

*Corresponding author. Tel: +86-25-89680373; Fax: +86-25-89680596.

*E-mail*: heyunfu@nju.edu.cn (H. Fu)

## Experimental section

### 1. Chemical and Materials

Analytical grade nickel (II) acetate tetrahydrate ($Ni(CH_3COO)_2•4H_2O$) and 2,5-dihydroxyterephthalic acid (DHTP) were purchased from Macklin Biochemical Co., Ltd., China. *N*,*N*-dimethylformamide (DMF, 99.9%), methanol and 1,2-dichloroethane (99.8%) were purchased from Aladdin Chemistry Co., Ltd., China. Methane, ethylene, ethane, hydrogen, nitrogen and helium gases were purchased from Tianze Gas Corporation, Nanjing, China. SBA-15 was obtained from Nanjing XFNANO Materials Tech Co., Ltd. All chemicals were used without further purification.

### 2. Catalysts preparation

*2.1 Synthesis of nano-sized Ni-MOF-74*

Nanosized Ni-MOF-74 was prepared according to the literature method.[1] Briefly, 0.2 g of DHTP was dissolved in 5.3 mL of DMF to form a clear yellow solution. Then the yellow solution was added dropwise into a solution containing 0.65 g of $Ni(CH_3COO)_2•4H_2O$ and 5.3 mL of DMF under continuous stirring. The mixture was further stirred at room temperature for 20 h. Then the nanocrystals were separated by centrifugation and washed with DMF and methanol. The yellow sample was obtained after drying under vacuum at 200$^{o}$C for 12 h.

*2.2 Synthesis of xNi-MOF-74@SBA-15*

A series of xNi-MOF-74@SBA-15 (x=1, 4, 17, where x represents theoretical Ni loading amount in the materials) hybrid materials were prepared by *in-situ* growth of nano-sized Ni-MOF-74 inside mesopores of SBA-15. For 1Ni-MOF-74@SBA-15, 500 mg of SBA-15 was mixed with 3.72 mL of DMF containing 0.065 g of $Ni(CH_3COO)_2•4H_2O$ and stirred for 30 min. Subsequently, another solution containing 0.02 g of DHTP and 0.53 mL of DMF was added dropwise into the above mixture. The mixture was then stirred for 20 h at room temperature. The solid product was isolated by filtration, washed with DMF and methanol for a few times and dried under vacuum at 200 $^oC$ for 12 h. The obtained material was denoted as 1Ni-MOF-74@SBA-15. Accordingly, 4Ni-MOF-74@SBA-15 and 17Ni-MOF-74@SBA-15 were prepared according to above-described procedure by increasing $Ni(CH_3COO)_2•4H_2O$ loading amount.

*2.3 Synthesis of Ni@PC*

Ni@PC was prepared by direct pyrolysis of pristine nano-sized Ni-MOF-74 at 450 $^oC$ for 8 h at a ramping rate of 10 $^oC\ min^{-1}$ under $N_2$ atmosphere.

*2.4 Synthesis of xNi-PC@SBA-15*

xNi-PC@SBA-15 was prepared by the direct pyrolysis of xNi-MOF-74@SBA-15 at 450 $^oC$ for 8 h under $N_2$ atmosphere using a quartz tubular reactor vertically located in an oven.

*2.5 Synthesis of 1Ni@SBA-15*

The 1Ni@SBA-15 was synthesized by calcination of 1Ni-PC@SBA-15 at 450 $^{o}$C for 2 h in air at a heating rate of 10 $^{o}$C min$^{-1}$.

*2.6 Synthesis of 1Ni/SBA-15*

1Ni/SBA-15 was prepared through the conventional impregnation method. Briefly, SBA-15 was impregnated with a required amount of $Ni(CH_3COO)_2 \cdot 4H_2O$ solution, followed by drying at 110 $^{o}$C for 4 h. The resulting material was calcinated under $N_2$ flow at 450 $^{o}$C for 8 h.

## 3. Catalysts Characterization

The Ni contents in the catalysts were determined by an inductively coupled plasma-atomic emission spectrometer (ICP-AES) (J-A1100, Jarrell-Ash, USA). The powder X-ray diffraction (XRD) measurements were performed on a Rigaku D/max-RA powder diffraction-meter (Rigaku, Tokyo, Japan) provided with Cu Kα radiation. Fourier Transform Infrared (FT-IR) spectra were collected at room temperature in the range 500-4000 cm$^{-1}$ on a Nexus 870 Spectrometer (Nicolet, USA) with a resolution of 4 cm$^{-1}$. The diffuse reflectance ultraviolet-visible (DR-UV/vis) spectra were obtained on SHIMADZU UV-2450 UV/vis spectrophotometer (Shimadzu Co., Kyoto, Japan) using $BaSO_4$ as the reference. The specific surface areas and average pore diameters of the materials were measured from $N_2$

adsorption/desorption isotherms at 77 K on a Micromeritics ASAP 2020 surface area analyzer (Micromeritics Instrument Co., USA). Prior to the measurements, the materials were degassed at 150 $^{o}$C for 8 h under vacuum. Morphologies of the catalysts were observed using scanning electron microscopy (SEM, S-3400N II, Hitachi, Japan) and transmission electron microscopy (TEM, JEOL Co., Japan). The surface compositions of the catalysts were analyzed by X-ray photoelectron spectroscopy (XPS, PHI-5000 VersaProbe, ULVAC-PHI, Japan). The binding energy was calibrated by measuring the C1s binding energy of 284.6 eV. Thermal decomposition of Ni-MOF-74 and xNi-MOF-74@SBA-15 were measured on a Pyris 1 thermalgravimetric analyzer (TGA, Perkin Elmer, USA). During analysis, the samples were heated from 30 to 700 $^{o}$C with a heating rate of 20 $^{o}$C min$^{-1}$ in a continuous $N_2$ atmosphere. Temperature programmed desorption of $H_2$ ($H_2$-TPD) analysis for 1Ni-PC@SBA-15 and 1Ni@SBA-15 was carried out in a fully automated AMI-300 catalyst characterization instrument (Altamira Instruments, USA) equipped with a thermal conductivity detector. About 60 mg of catalyst was placed in a U-shaped quartz tube inside an electrical furnace and pretreated at 150 $^{o}$C for 60 min under He stream. After cooling to room temperature, the catalyst was reduced in situ at 450 $^{o}$C for 2 h in a 10% $H_2$/Ar flow and then cooled to 30 $^{o}$C. The catalyst was exposed to 10% $H_2$/Ar for 30 min, swept with He for 30 min to remove the physically adsorbed $H_2$. $H_2$-TPD was performed by ramping to 600 $^{o}$C at a rate of 10 $^{o}$C min$^{-1}$.

## 4. Gas phase catalytic HDC of 1,2-dichloroethane

Gas phase catalytic HDC of 1,2-dichloroethane was conducted in a continuous fixed-bed quartz tubular reactor at 300 $^{o}$C under atmospheric pressure. Typically, 50 mg of catalyst sieved to 20-40 mesh was loaded between two layers of quartz wool. Prior to the catalytic HDC, the catalyst was reduced at 400 $^{o}$C for 2 h in $H_2$ with a flow rate of 30 ml $min^{-1}$. After cooling to 300 $^{o}$C, 1,2-dichloroethane was injected at 0.025 ml $h^{-1}$ using an infusion pump controlled by a microprocessor into a mixed gas flow (42 ml $min^{-1}$), which consisted of $H_2$ and a balance of He (He:$H_2$=40.7mL:1.3mL). The reaction products were analyzed using a gas chromatography equipped with a flame ionization detector (GC-FID).

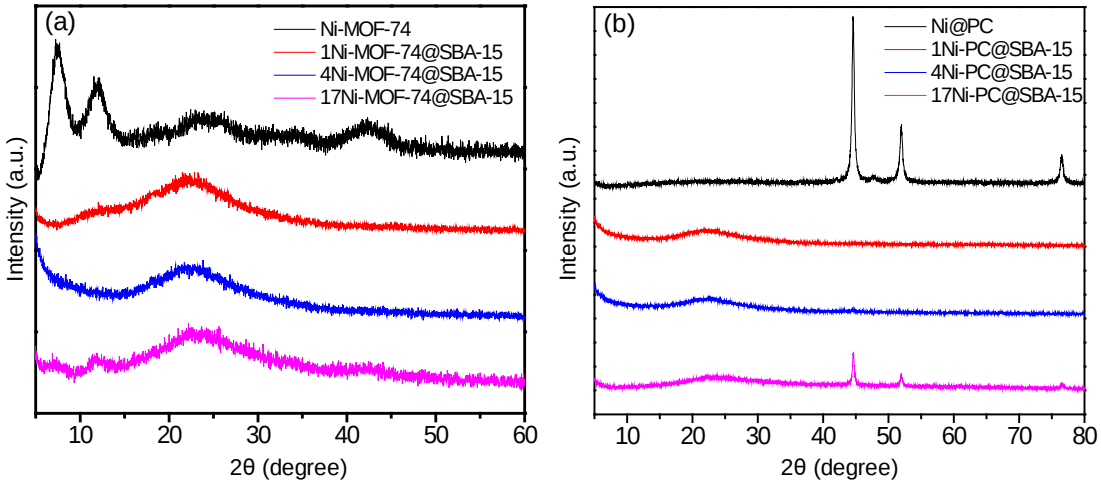


**Fig. S1.** XRD patterns of (a) nano-sized Ni-MOF-74 and xNi-MOF-74@SBA-15 and (b) Ni@PC and xNi-PC@SBA-15.

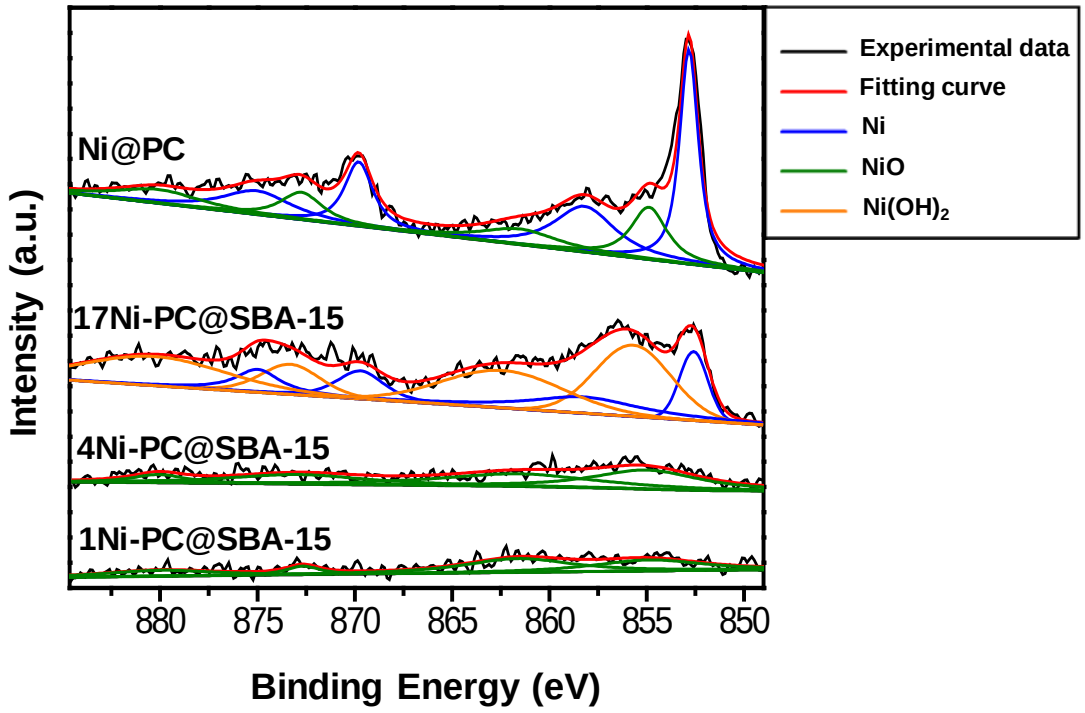


**Fig. S2.** Ni 2p XPS spectra of different Ni-based catalysts.

The Ni $2p_{3/2}$ peak at 852.6 eV and $2p_{1/2}$ peak at 869.7 eV and two intensive shake-up satellites with binding energy at 858.2 and 875.0 eV were corresponding to metallic Ni.[2] The Ni $2p_{3/2}$ peak at 854.9 eV with a satellite peak around 861.6 eV and the $2p_{1/2}$ peak at 872.7 eV with a satellite peak around 880.1 eV were assigned to NiO.[2] Ni $2p_{3/2}$ peak at 855.7 eV with a satellite at 862.4 eV and $2p_{1/2}$ peak at 873.3 eV a satellite at 880.3 eV were attributed to $Ni^{2+}$ from $Ni(OH)_2$. The presence of NiO and $Ni(OH)_2$ was likely due to easy oxidation of surface metallic Ni when exposed to air.[2c] In comparison with 17Ni-PC@SBA-15 and Ni@PC, metallic Ni was not detected in 1Ni-PC@SBA-15 and 4Ni-PC@SBA-15, attributing to very small Ni particles which were prone to oxidation upon exposure to air.[3] In parallel, the majority of Ni species were in the form of metallic Ni in Ni@PC because of its large Ni particle size.

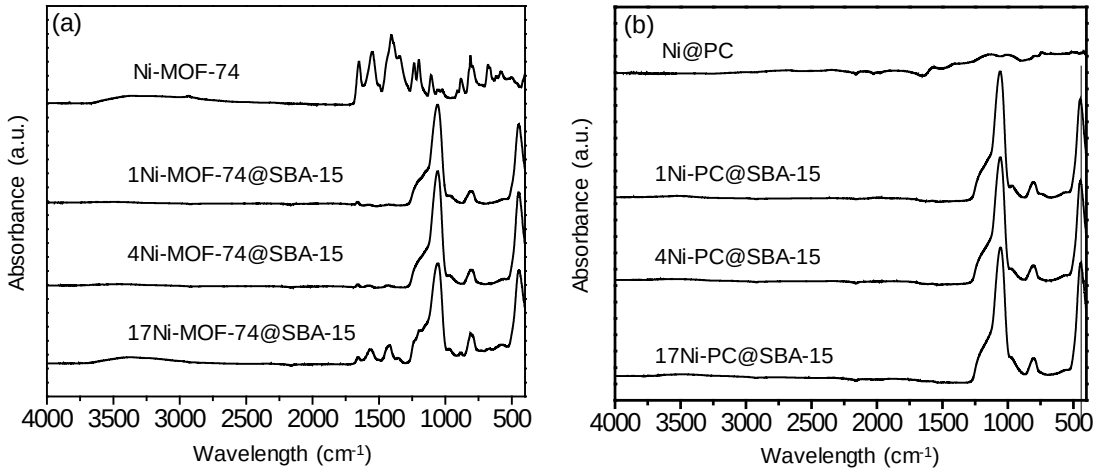


**Fig. S3.** IR spectra of (a) nano-sized Ni-MOF-74 and xNi-MOF-74@SBA-15 and (b) Ni@PC and xNi-PC@SBA-15.

The IR spectrum of Ni@PC in Fig. S3b showed no distinct peaks characteristic of Ni-MOF-74, suggesting the complete decomposition of nano-sized Ni-MOF-74. For xNi-PC@SBA-15, the bands were mainly related to the $SiO_2$. The band around 3500 $cm^{-1}$ was assigned to the hydrated silanol groups. Two peaks at 1056 and 800 $cm^{-1}$ were characteristic of Si-O asymmetric and symmetric stretching vibrations from the $SiO_2$.[4] The bands at 966 and 450 $cm^{-1}$ were attributed to Si-O stretching and O-Si-O bending vibration mode of surface silanol groups.[5]

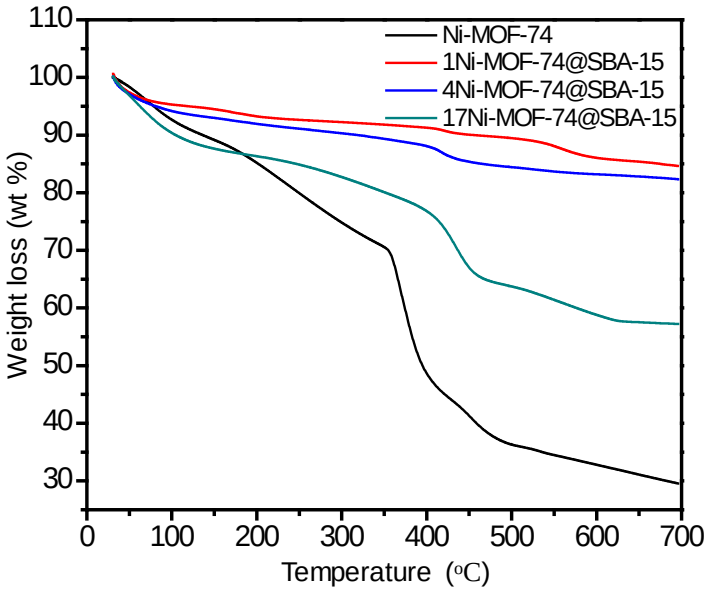


**Fig. S4.** TGA curves of Ni-MOF-74 and xNi-MOF-74@SBA-15.

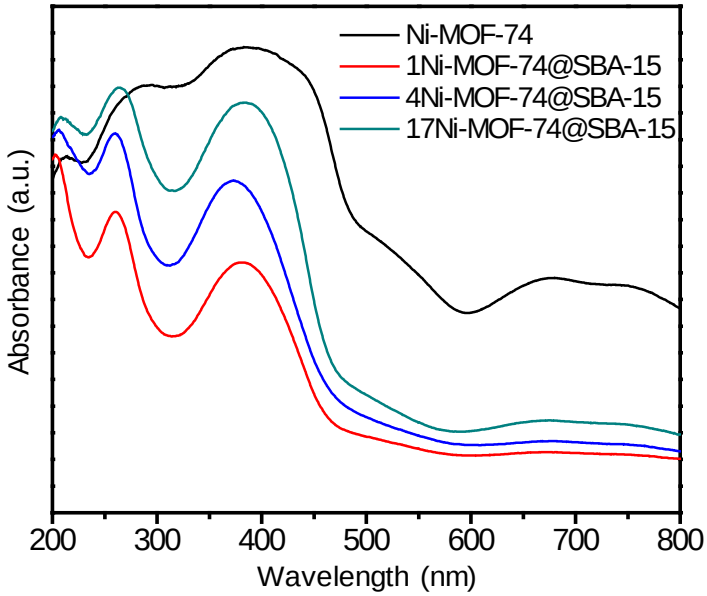


**Fig. S5.** DR-UV/Vis spectra of nano-sized Ni-MOF-74 and xNi-MOF-74@SBA-15.

Both pristine nano-sized Ni-MOF-74 and xNi-MOF-74@SBA-15 exhibited the typical DR-UV/Vis spectra of MOF-74.[6,7] The weak band at 210 nm with a shoulder peak at 275 nm was associated with $O^{2-}$-$Ni^{2+}$ electron charge transfer.[6] The absorbance peaks at 407, 665 and 740 nm are related to mononuclear $Ni^{2+}$ ions in octahedral coordination.[7] Two absorbance peaks at 407 and 740 nm are attributed to spin-allowed electron transfer transition $^3A_{2g}$ (F)→$^3T_{1g}$ (P) and $^3A_{2g}$ (F) →$^3T_{1g}$ (F), respectively, and a band at 665 nm to spin-forbidden one.[7]

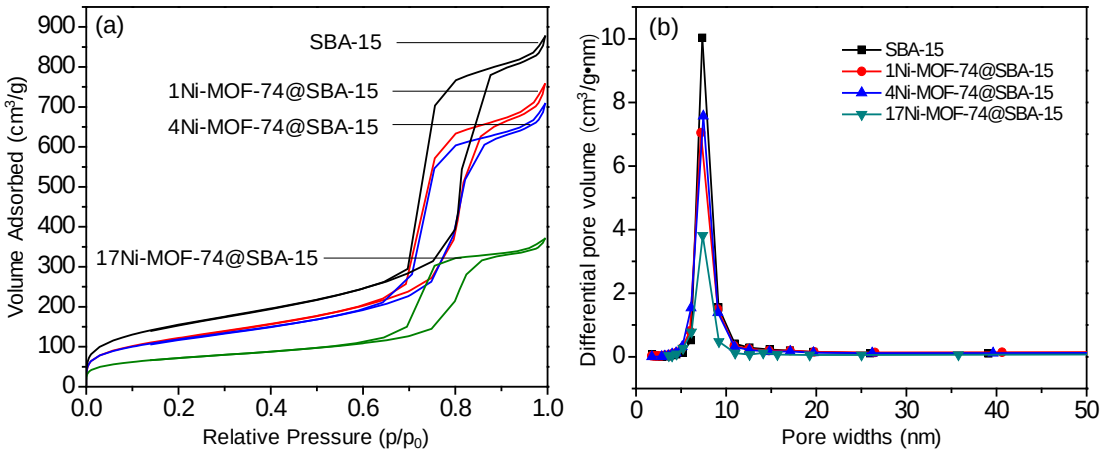


**Fig. S6.** The (a) $N_2$ adsorption-desorption isotherms and (b) pore size distributions of SBA-15 and xNi-MOF-74@SBA-15.

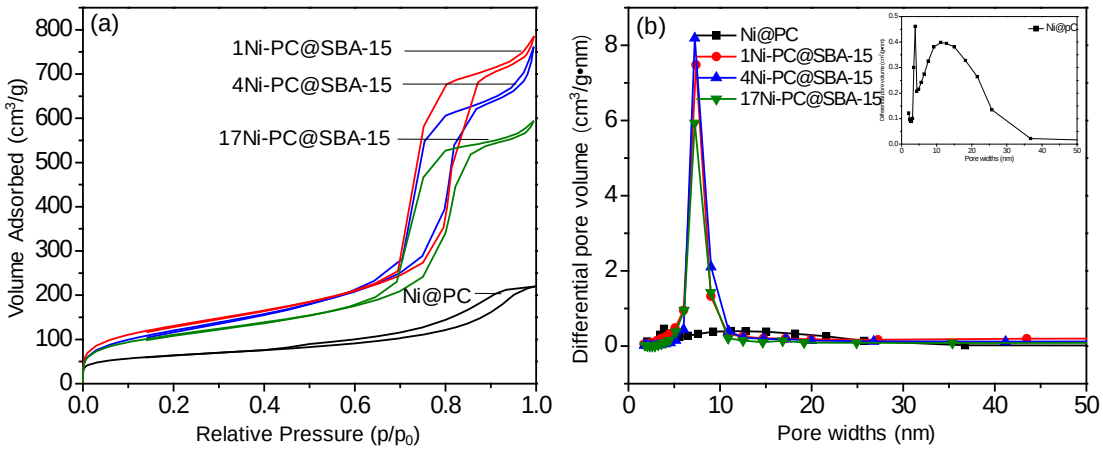


**Fig. S7.** The (a) $N_2$ adsorption-desorption isotherms and (b) pore size distributions of different Ni-based catalysts.

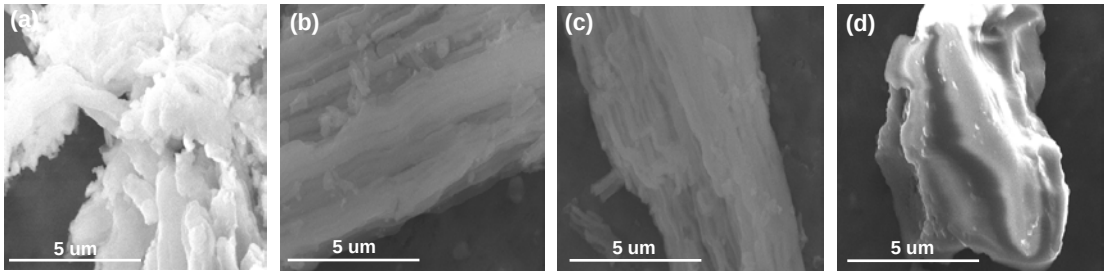


**Fig. S8.** SEM images of (a) nano-sized Ni-MOF-74, (b) 1Ni-MOF-74@SBA-15, (c) 4Ni-MOF-74@SBA-15 and (d) 17Ni-MOF-74@SBA-15.

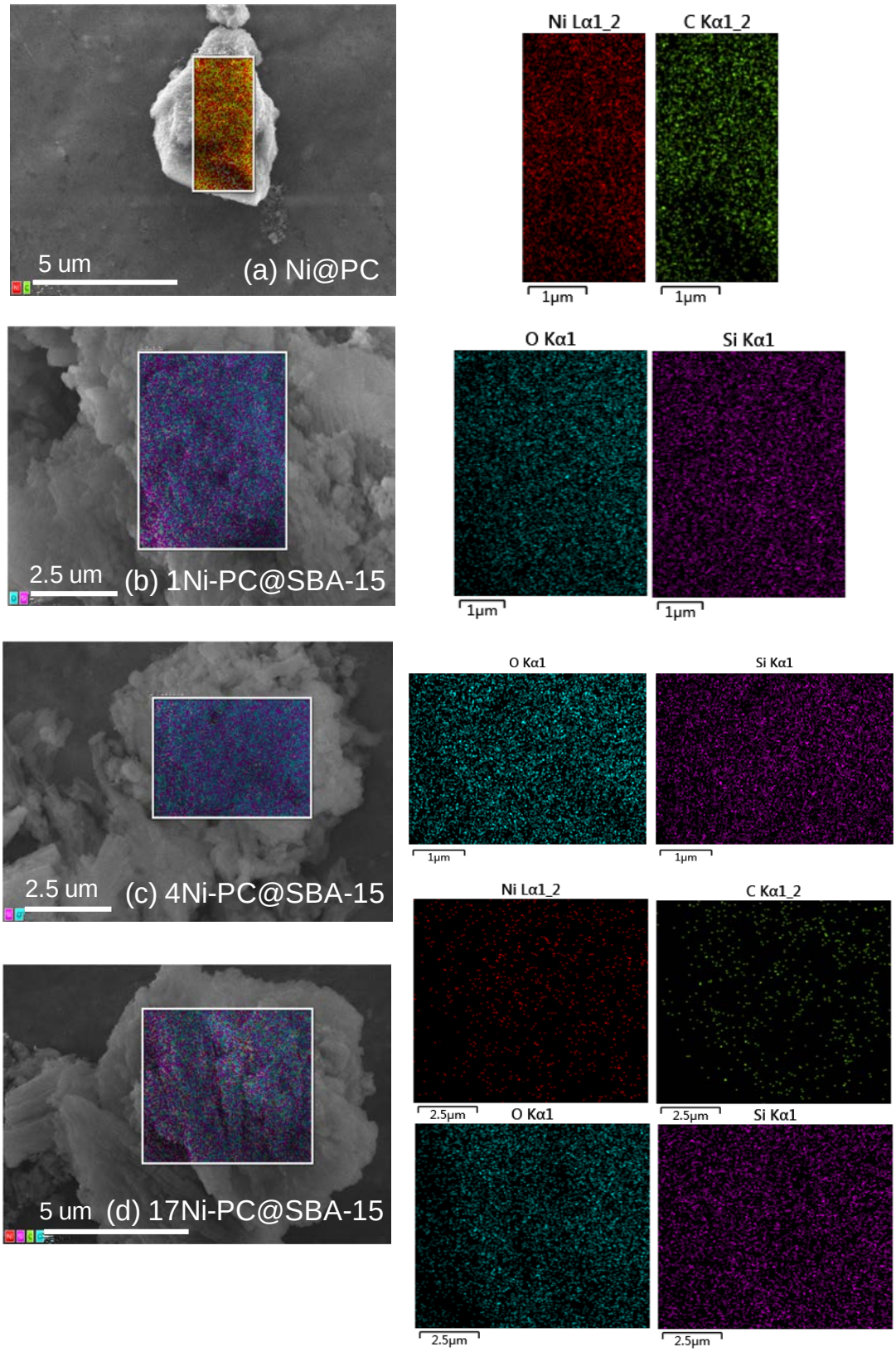


**Fig. S9.** SEM images and elemental mapping of different Ni-based catalysts.

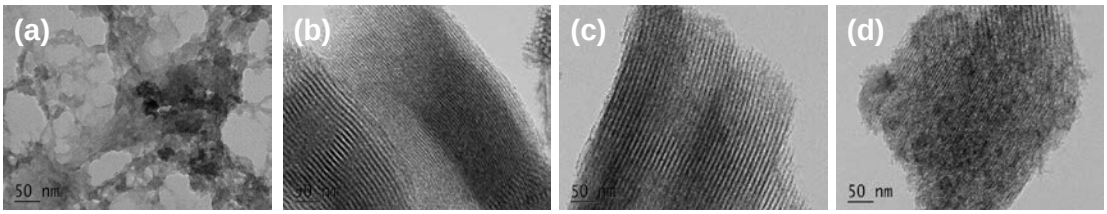


**Fig. S10.** TEM images of (a) nano-sized Ni-MOF-74, (b) 1Ni-MOF-74@SBA-15, (c) 4Ni-MOF-74@SBA-15 and (d) 17Ni-MOF-74@SBA-15.

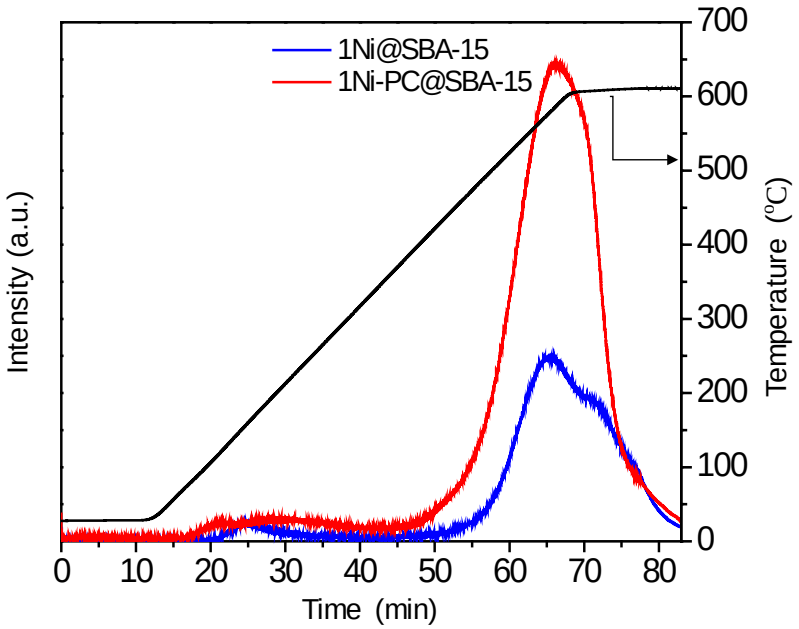


**Fig. S11.** $H_2$-TPD profiles of 1Ni-PC@SBA-15 and 1Ni@SBA-15.

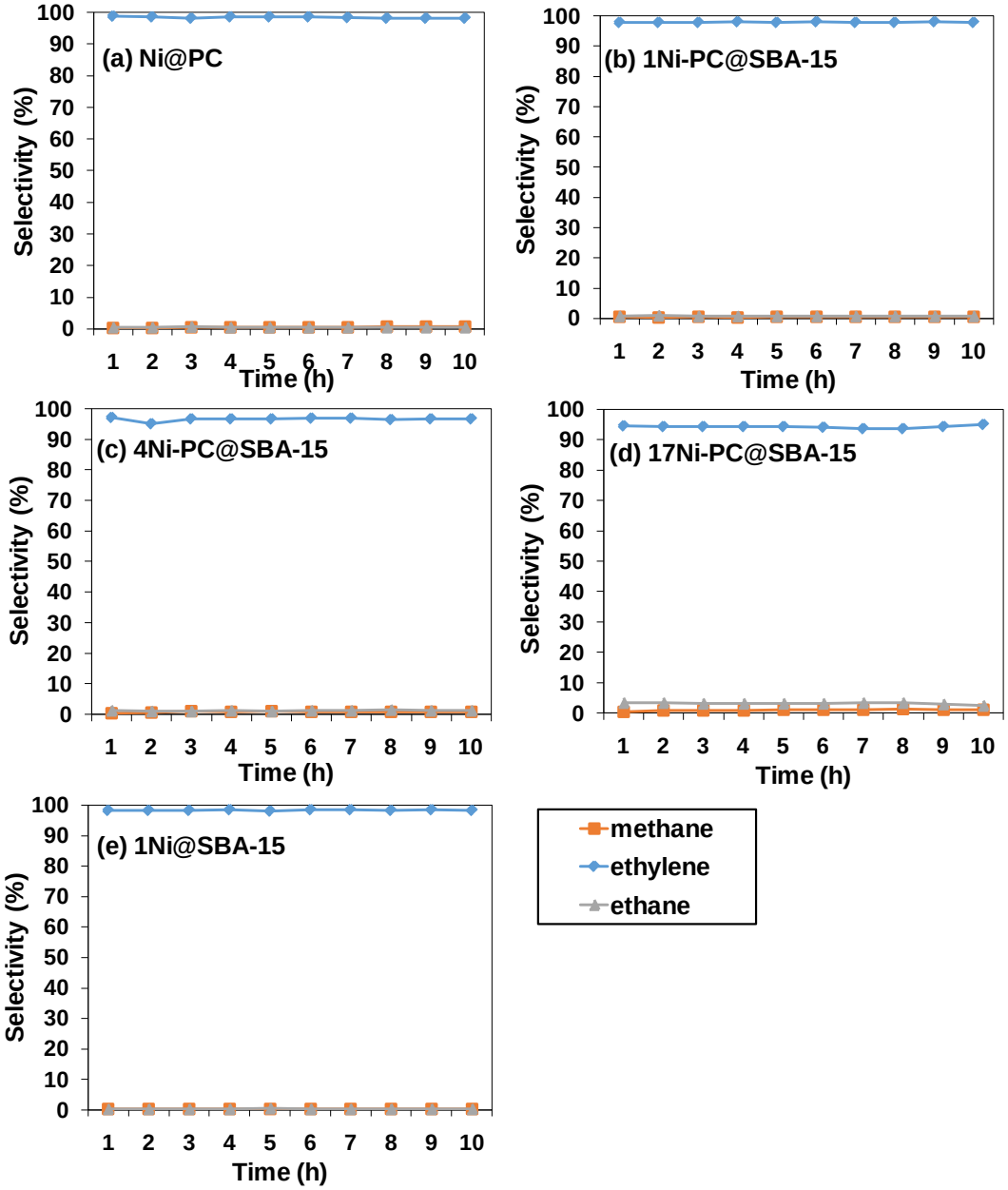


**Fig. S12.** The selectivity as a function of time on stream for the gas phase catalytic hydrodechlorination of 1,2-dichloroethane over different Ni-based catalysts.

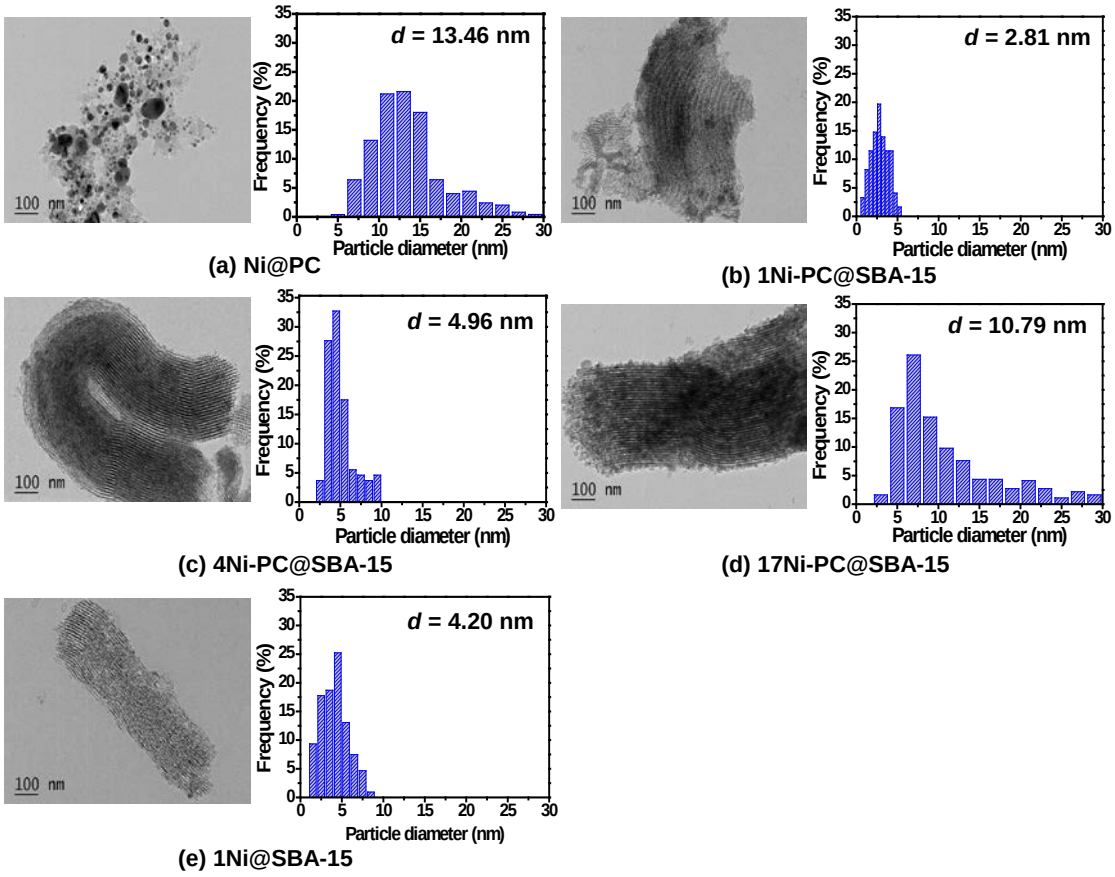


**Fig. S13.** The TEM images and Ni particles size distribution of Ni-based catalysts after use.

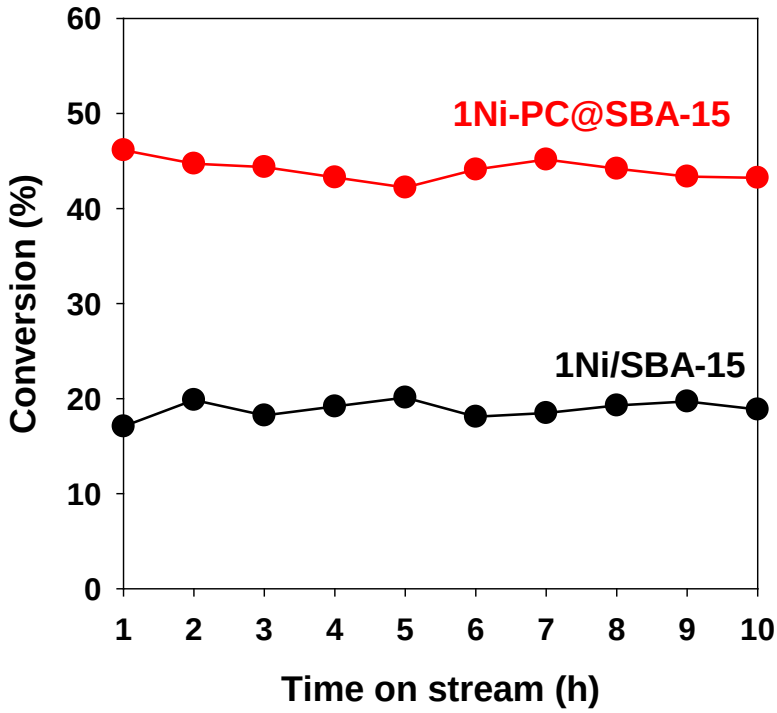


**Fig. S14.** Conversion as a function of time on stream for gas phase catalytic hydrodechlorination of 1,2-dichloroethane over 1Ni-PC@SBA-15 and 1Ni/SBA-15.

**Table S1.** Structural properties and catalytic activities of different Ni-based catalysts.

| Sample | Ni content [a] (wt.%) | Ni particle size [b] (nm) | Ni dispersion [c] (%) | BET surfaces area [d] ($m^2/g$) | Pore volume [d] ($cm^3/g$) | Pore diameter [d] (nm) | TOF ($h^{-1}$) |
|---|---|---|---|---|---|---|---|
| Ni@PC | 73.66 | 11.88 | 8.14 | 214.79 | 0.33 | 7.10 | 2.64 |
| 1Ni-PC@SBA-15 | 0.89 | 2.45 | 39.47 | 415.30 | 1.22 | 8.27 | 42.04 |
| 4Ni-PC@SBA-15 | 4.24 | 4.37 | 22.13 | 420.59 | 1.18 | 8.09 | 21.83 |
| 17Ni-PC@SBA-15 | 17.0 | 9.88 | 9.79 | 379.93 | 0.93 | 7.78 | 14.41 |
| 1Ni@SBA-15 | 0.91 | 2.80 | 34.54 | 440.82 | 1.21 | 8.17 | 28.86 |

[a] Determined by ICP-AES.

[b] Calculated from TEM.

[c] Calculated according to dispersion (%) = $96.7/d_s$ (nm), where $d_s$ is the surface area weighted diameter of Ni particles.

[d] Determined by $N_2$ adsorption/desorption isotherms at 77 K.

**Table S2.** Surface area and pore volume parameters of SBA-15 and xNi-MOF-74@SBA-15.[a]

| Sample | BET surface area ($m^2/g$) | Pore volume ($cm^3/g$) | Pore diameter (nm) |
|---|---|---|---|
| SBA-15 | 535.04 | 1.37 | 8.09 |
| 1Ni-MOF-74@SBA-15 | 424.21 | 1.18 | 8.16 |
| 4Ni-MOF-74@SBA-15 | 409.15 | 1.10 | 8.20 |
| 17Ni-MOF-74@SBA-15 | 244.55 | 0.58 | 8.05 |

[a] Determined by $N_2$ adsorption/desorption isotherms at 77 K.

**Notes and references**


1. M. Díaz-García, Á. Mayoral, I. Díaz and M. Sánchez-Sánchez, *Cryst. Growth Des.*, 2014, **14**, 2479-2487.
2. (*a*) C. Li, A. Proctor and D. Hercules, *Appl. Spectrosc.*,1984, **38**, 880-886. (*b*) W. Lin, H. Cheng, J. Ming, Y. Yu and F. Zhao, *J. Catal.*, 2012, **291**, 149-154. (*c*) J. Xia, G.He, L. Zhang, X.Sun and X.Wang, *Appl. Catal., B*, 2016,**180**, 408-415.
3. K. Sato, F. Sago, K. Nagaoka and Y. Takita, *Int. J. Hydrogen Energ.*, 2010, **35**, 5393-5399.
4. H. Veisi, D. Kordestani and A. Faraji, *J. Porous Mater.*, 2014, **21**, 141-148.
5. V. Brahmkhatri and A. Patel, *Appl. Catal. A: Gen.*, 2011, **403**, 161-172.
6. S. Damyanova, B. Pawelec, K. Arishtirova and J.L.G. Fierro, *Int. J. Hydrogen Energ.*, 2012, **37**, 15966-15975.
7. J. Villajos, G. Orcajo, C. Martos, J. Botas, J. Villacañas and G. Calleja, *Int. J. Hydrogen Energ.*, 2015, **40**, 5346-5352.